


RESEARCH ARTICLE

Disruptions of frontoparietal control network and default mode network linking the metacognitive deficits with clinical symptoms in schizophrenia

Wenbin Jia¹ | Hong Zhu² | Yinmei Ni¹ | Jie Su¹ | Rui Xu² | Hongxiao Jia² | Xiaohong Wan¹ 

¹State Key Laboratory of Cognitive Neuroscience and Learning and IDG/McGovern Institute for Brain Research, Beijing Normal University, Beijing, China

²National Clinical Research Center for Mental Disorders & Beijing Key Laboratory of Mental Disorders and Beijing Anding Hospital, Capital Medical University, Beijing, China

Correspondence

Xiaohong Wan, State Key Laboratory of Cognitive Neuroscience and Learning IDG/McGovern Institute for Brain Research, Beijing Normal University, Beijing 100875, China.
Email: xhwan@bnu.edu.cn

Hongxiao Jia, National Clinical Research Center for Mental Disorders & Beijing Key Laboratory of Mental Disorders and Beijing Anding Hospital, Capital Medical University, Beijing 100088, China.
Email: jhxhj@vip.163.com

Funding information

Key Program for International S&T Cooperation Projects of China, Grant/Award Number: 2016YFE0129100; National Natural Science Foundation of China, Grant/Award Number: 31471068; the Fundamental Research Funds for the Central Universities, Grant/Award Number: 2017EYT33

Abstract

The metacognitive deficit in awareness of one's own mental states is a core feature of schizophrenia (SZ). The previous studies suggested that the metacognitive deficit associates with clinical symptoms. However, the neural mechanisms underlying the relationship remain largely unknown. We here investigated the neural activities associated with the metacognitive deficit and the neural signatures associated with clinical symptoms in 38 patients with SZ using functional magnetic resonance imaging with a perceptual decision-making task accompanied with metacognition, in comparison to 38 age, gender, and education matched healthy control subjects. The metacognitive deficit in patients with SZ was associated with reduced regional activity in both the frontoparietal control network (FPCN) and the default mode network. Critically, the anticorrelational balance between the two disrupted networks was substantially altered during metacognition, and the extent of alteration positively scaled with negative symptoms. Conversely, decoupling between the two networks was impaired when metacognitive monitoring was not required, and the strength of excessive neural activity positively scaled with positive symptoms. Thus, disruptions of the FPCN and the default mode network underlie the metacognitive deficit, and alternations of network balance between the two networks correlate with clinical symptoms in SZ. These findings implicate that rebalancing these networks holds important clinical potential in developing more efficacious therapeutic treatments.

KEYWORDS

dACC, decision uncertainty, fMRI, metacognition, network imbalance, PCC, schizophrenia

1 | INTRODUCTION

The lack of awareness of one's own mental states, such as suffering mental illness and pathologic mental experiences, has been widely recognized as an invariable feature of patients of schizophrenia

(SZ) (Amador, Strauss, Yale, & Gorman, 1991; Carpenter, Strauss, & Bartko, 1973). This clinically significant feature is associated with both negative and positive symptoms and cognitive dysfunctions (Amador et al., 1993; Smith et al., 2000; Lysaker & Bell, 1994; Green, 1996), and also predicts functional outcomes after treatments (Lincoln et al., 2006; Robinson, Woerner, McMeniman, Mendelowitz, & Bilder, 2004). Awareness of one's own mental states has been broadly

Wenbin Jia, Hong Zhu, Yinmei Ni are co-first authors.

This is an open access article under the terms of the Creative Commons Attribution-NonCommercial License, which permits use, distribution and reproduction in any medium, provided the original work is properly cited and is not used for commercial purposes.

© 2019 The Authors. *Human Brain Mapping* published by Wiley Periodicals, Inc.

referred to as metacognition (Dunlosky & Metcalfe, 2009; Flavell, 1979; Nelson & Narens, 1990). Although there have existed many clinical studies on the metacognitive deficits in SZ, a lack of operational definition of metacognitive deficits makes it difficult to use a proper experimental paradigm to investigate the underlying neural mechanisms. To date, there are growing interests in neuroscience to investigate neural mechanisms of metacognition (Fleming, Huijgen, & Dolan, 2012; Kiani & Shadlen, 2009; Miyamoto et al., 2017; Morales, Lau, & Fleming, 2018). Nevertheless, the neural accounts linking the metacognitive deficits and clinical symptoms in SZ remain largely obscure (Buchy, Stowkowy, MacMaster, Nyman, & Addington, 2015; Francis et al., 2017).

A characteristic trait of SZ is overconfidence (Beck, Baruch, Balter, Steer, & Warman, 2004; Moritz & Woodward, 2006). They often report higher levels of confidence for incorrect responses than healthy control subjects (HC) (Danion, Gokalsing, Robert, Massin-Krauss, & Bacon, 2001). Overall, they display larger divergences between confidence ratings and actual accuracy of task performance. Thus, the metacognitive deficit in monitoring decision uncertainty (or decision confidence) is prominent in SZ. Opposing to decision confidence, decision uncertainty is regarded as the level of subjective belief that the decision could be incorrect. In terms of the cognitive control framework (Nelson & Narens, 1990), decision uncertainty, rather than decision confidence, is the key signal that elicits metacognition immediately accompanying decision-making. When there is no uncertainty regarding the preceding decision, the subsequent processes of metacognitive control should be not evoked. In contrast, when the decision uncertainty is high, the metacognitive processes should be evoked to revise the preceding decision. Several recent studies using functional MRI (fMRI) in simple perceptual decision-making tasks have shown that the frontoparietal control network (FPCN) and the salience network (SN) are associated with metacognition accompanying the decision-making task in the population of HC (Fleming et al., 2012; Morales et al., 2018; Qiu et al., 2018; Wan, Cheng, & Tanaka, 2016). The fMRI activities in these regions increase as decision uncertainty increases. Specifically, the fMRI activities in the dorsal anterior cingulate cortex (dACC) positively scale with individual metacognitive ability of uncertainty monitoring (Qiu et al., 2018). Furthermore, the same network is also involved in metacognitive control of decision adjustment (Qiu et al., 2018; Wan et al., 2016). Therefore, metacognition is associated with the FPCN and SN, together referred to as "the metacognition network" (MCN). Meta-analyses of structural and resting-state fMRI studies have showed that the anatomical volumes and intrinsic fMRI activities in these regions are consistently less in SZ than HC (Pettersson-Yeo, Allen, Benetti, McGuire, & Mechelli, 2011; Goodkind et al., 2015; Brugger & Howes, 2017). Hypo-activity in these regions has prevalently been observed during tasks that required error or conflict monitoring (Carter, MacDonald, Ross, & Stenger, 2001; Kerns et al., 2005). Thus, the metacognitive deficit in SZ could be associated with hypo-activity in the MCN.

It has been also suggested that reduced suppression of the default mode network (DMN) during task performing is related to

the neuropathology of SZ (Metzak et al., 2012; Whitfield-Gabrieli et al., 2009). However, reduction of the DMN suppression could be induced by hypo-activity in the MCN in SZ, as the DMN activity always anticorrelates with the MCN activity (Fox, Snyder, Vincent, Corbetta, & Raichle, 2005; Gusnard & Raichle, 2001). The DMN regions are proportionally suppressed while the MCN regions are activated during metacognition (Qiu et al., 2018). Indeed, the DMN suppression is even elevated in some SZ patients (Harrison, Yücel, Pujol, & Pantelis, 2007; Mannell et al., 2010). Thus, the metacognitive deficit in SZ could be also associated with reduction of the DMN suppression.

While the MCN and DMN are proposed as the preferential networks showing disruptions in SZ (Anticevic et al., 2012; Yang et al., 2016), thus far, no study has articulated the critical feature of the two networks that reliably associate with clinical symptoms. Utilizing an established experimental paradigm of a simple perceptual decision-making task (Qiu et al., 2018), our goals in this study were to test the two hypotheses in SZ: (a) suppression of activities in both the MCN and DMN is associated with the metacognitive deficit in decision uncertainty monitoring, and (b) alternations of the two disrupted networks are associated with clinical symptoms.

2 | METHODS

2.1 | Subjects

Demographic data for the study are provided in Table 1. The SZ ($n = 38$) and HC ($n = 38$) groups did not significantly differ in age, gender or education distribution. Exclusion criteria included: a current diagnosis of

TABLE 1 Subjects' demographic, clinical, and self-report measures

	HC ($n = 38$)		SZ ($n = 38$)		t (χ^2)	P^a
	Mean	SD	Mean	SD		
Demographic						
Age (y)	23	4.6	22.6	8.3	0.38	0.71
Gender (male)	20	-	23	-	0.48	0.49
Education (y)	13.2	1.3	13	3.1	0.48	0.63
Illness (m)	-	-	37.5	47.9	-	-
Medication ^b	-	-	369	397	-	-
PANSS ^c						
Positive	-	-	13.2	5.6	-	-
Negative	-	-	14.1	6.4	-	-
General	-	-	27.2	5.4	-	-
Total	-	-	54.6	12.9	-	-

^aThe difference between HC and SZ, P values correspond to two-sample two-tailed t -tests for continuous variables and χ^2 for categorical variables.

^bIf patients were receiving medications, we converted individual patient medication levels to chlorpromazine equivalents via standard approaches.

^cPositive and Negative Syndrome Scale.

substance abuse, neurological disorder, or head trauma. Clinical assessment was performed at the time of screening, using the positive and negative symptoms scores (PANSS) (Kay, Fiszbein, & Opler, 1987). All patients were being treated with antipsychotics at the time of the study. Informed consent was obtained from each individual participant in accordance with a protocol approved by Beijing Normal University Research Ethics Committee (ICBIR_A_0091_002).

2.2 | Task paradigm

We employed the “decision-redecision” paradigm that detailed in a previous study (Qiu et al., 2018). Briefly, the subject was instructed to make an initial decision regarding the moving direction of a random-dot-motion (RDM) stimulus (decision phase), and then was required to immediately make a second decision on the same stimulus (redcision

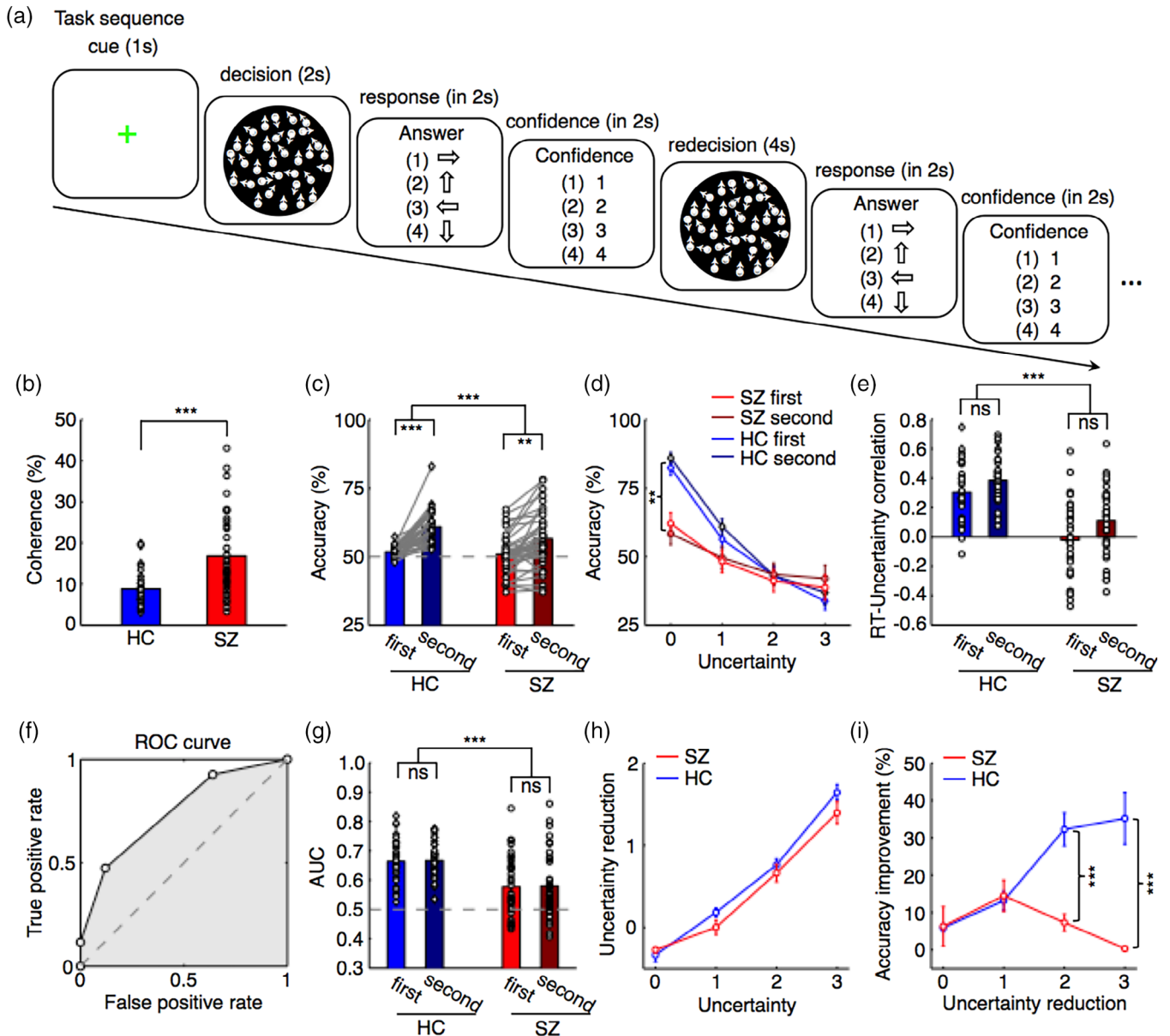


FIGURE 1 The experimental paradigm and behavioral performance. (a) The task sequence of the “decision-redecision” paradigm to make decisions twice on the same stimulus. (b) Significant difference of the mean stimulus coherence between HC and SZ. (c) The performance accuracy was controlled to 50% in the first decision-making for both groups, while the accuracy improvement by redcision was significantly different between HC and SZ. (d) The performance accuracy was reversely proportional to the decision uncertainty levels in HC, but not in SZ. (e) The correlation coefficients between RT and decision uncertainty in both phases were significantly different between HC and SZ. (f) The receiver-operating characteristic (ROC) constructed using the decision uncertainty levels as judgment criteria. The shading area represents the area under the curve (AUC). (g) The behavioral uncertainty sensitivities (b-AUC) in both phases were significantly different between HC and SZ. The dotted line represents the chance level (0.5). (h) The uncertainty reduction by redcision was positively correlated with the decision uncertainty level on the first decision for both groups. (i) Accuracy improvement at higher levels of decision uncertainty reduction in HC was significantly higher than that in SZ. ns, no significance; * $p < .05$, ** $p < .01$, *** $p < .001$. Error bars indicate standard error of mean across subjects

phase). The mental state of uncertainty regarding the first and second decisions was separately evaluated by confidence ratings. The subject reported his/her confidence level from 1 (most uncertain) to 4 (most certain) by pressing a corresponding button. The level of decision uncertainty was thus the opposite of the confidence rating [a confidence rating of 4 (1) corresponds to a decision uncertainty level of 0 (3)]. The task difficulty of each trial was adaptively adjusted by a staircase procedure (Levitt, 1971), so that the overall accuracy of the first decisions for each subject converged to approximately 50% (the chance level = 25%).

In each trial, after the stimulus was presented for 2 s, the subject made a choice from the four-presented choice options within 2 s, and reported a confidence rating for that decision within 2 s (Figure 1a). The same stimulus was then immediately presented again for 4 s, and the subject made a choice and reported a confidence rating again each within 2 s. After the subject made a response or the current response phase ran out of 2 s, the task sequence immediately went to the next phase. No feedback was provided after either the first or second decision-making. In the control condition, the subject reported a decision on an unambiguous RDM directional stimulus for which there was 100% coherence of movement direction. Totally there were 120 task trials and 40 control trials, randomly intermingled in four consecutive runs.

The RDM stimuli were 300 white dots (radius: 0.08° , density: 2.0%) that were presented on a black background. Typically, these dots were moving toward different directions with a speed of $8.0^\circ/s$ in an aperture with the radius of three degrees (visual angle). The lifetime of each dot lasted three frames. Some of the dots were moving toward the same direction (left, down, right or up), but the others were moving toward different random directions. The subject was required to discriminate the net motion direction. The stimulus coherences varied from 1% to 52% with the step size of 1%, whereas the coherence of moving dots in the control condition was 100%.

2.3 | Behavioral data analyses

To quantify the metacognitive ability of uncertainty monitoring in the task for each individual subject, a nonparametric approach was employed to construct the receiver operating characteristic (ROC) curve by characterizing the probability of incorrect decisions using different decision uncertainty levels as criteria (Figure 1f). The area under the curve of ROC (AUC) was measured to represent the behavioral uncertainty sensitivity (b-AUC).

2.4 | fMRI data acquisition and preprocessing

All fMRI experiments were conducted using a 3-T scanner (Siemens, Germany) with a 12-channel head coil. Functional images were acquired with a single-shot gradient-echo sequence with a volume repetition time of 2 s, echo time of 30 ms, slice thickness of 3.0 mm and in-plane resolution of $3.0 \times 3.0 \text{ mm}^2$ (field of view:

$19.2 \times 19.2 \text{ cm}^2$; flip angle: 90°). Thirty-eight axial slices were taken, with interleaved acquisition, parallel to the anterior commissure-posterior commissure line.

The analyses were conducted with the FMRIB Software Library (Smith et al., 2004). To correct for head motion, all functional images were realigned to the first volume of the first scan. Data sets in which the translation motions were larger than 2.0 mm or the rotation motions were larger than 1.0° were discarded. It turned out that no data had to be discarded in the fMRI experiments and no differences of head motions between the two groups (two-tailed two-sample *t* test, $t_{76} = 0.29$, $p = .41$). The functional images were first aligned to individual high-resolution structural images, and were then transformed to the Montreal Neurological Institute space using affine registration with 12° of freedom and data resampling at a resolution of $2 \times 2 \times 2 \text{ mm}^3$. Spatial smoothing with a 4-mm Gaussian kernel (full width at half-maximum) and high-pass temporal filtering with a cutoff of 0.005 Hz were applied to all fMRI data.

2.5 | fMRI data analyses

2.5.1 | Whole-brain analyses

In the general linear modeling (GLM) analyses, each trial was modeled with two regressors: (a) the first regressor representing the first decision-making was time-locked to the onset of the first stimuli presentation with the summation of the presentation time and the response time (RT) as the event duration; (b) the second regressor representing the metacognition phase (redecision) was time-locked to the onset of the first confidence judgment with the summation of the confidence report, the second presentation time of the stimuli and the RT of the choice.

To remove the confounding effect of RT from the neural correlates of decision uncertainty, the decision uncertainty level was first regressed out of RT. The residual was then implemented as the modulator of each regressor. The regressors were convolved with the canonical two-gamma hemodynamic response function (HRF). The head motion parameters, and the types and doses of antipsychotic medications in SC were added as covariates in the GLM analyses. For the group-level analyses, we used FMRIB's local analysis of mixed effects. Statistical parametric maps were generated using a threshold with $z = 3.1$, $p < .05$ with a false discovery rate (FDR) correction, unless noted otherwise.

To test whether it is still feasible to separate the mean activities and the decision uncertainty modulation effects between the two continuous phases, we made analyses on the simulation data that were generated from the exact same design matrix used for the subjects. The simulation data were created by the generative model as follows

$$y_{\text{bold}} = (\beta_1 + \beta_2 \times \text{uncertainty}) \times X_{\text{decision}} \otimes \text{hrf} + (\beta_3 + \beta_4 \times \text{uncertainty}) \times X_{\text{redecision}} \otimes \text{hrf} + \epsilon, \quad (1)$$

where X_{decision} and $X_{\text{redecision}}$ were the design matrix for the first decision-making and redecision phases, respectively. β_1 is the mean activity and β_2 is the decision uncertainty modulation effect in the

first decision-making phase, while β_3 is the mean activity and β_4 is the decision uncertainty modulation effect in the redecision phase. ϵ is an additional noise. The values of β_1 and β_3 , as well as β_2 or β_4 were independently and randomly drawn from a uniform distribution in the range of [0.2,0.8], while the complementary β_2 or β_4 was set to a small value as 10^{-5} . The signal-to-noise (SNR) varied from 0.01 to 1. We then used the same model to reconstruct the mean activities and the decision uncertainty modulation effects in the two phases. For each set of the parameters, 1,000 times were repeated and the estimated values were averaged (Figure 2).

2.5.2 | Regions-of-interest analyses

The regions-of-interest (ROIs) of the MCN and DMN were defined by the voxels that were significantly regressed with the decision uncertainty levels in an independent study (Qiu et al., 2018). These regions of the MCN and DMN complied with the locations of the two networks by the other studies (e.g., Yeo et al., 2011). The time courses associated with decision uncertainty were obtained using a GLM analysis on the trial-by-trial time courses (Figure 4a) (Behrens, Woolrich, Walton, & Rushworth, 2007; Qiu et al., 2018).

2.5.3 | Neural uncertainty sensitivity

In each ROI of each individual subject, each trial was independently modeled using a single regressor during the redecision phase convolved with the canonical HRF, and thus the β value of each trial was estimated (Mumford, Turner, Ashby, & Poldrack, 2012; Rissman,

Gazzaley, & D'Esposito, 2004). As the trial-by-trial neural activity strength was highly correlated with the decision uncertainty level (Qiu et al., 2018), the neural ROC curve was then constructed by characterizing the probability of incorrect decisions using different β values as criteria, likewise the computation of behavioral uncertainty sensitivity. The AUC was measured to represent the neural uncertainty sensitivity (n-AUC), as the approach to measuring the perceptual sensitivity of each individual MT neuron in animal studies (Britten, Shadlen, Newsome, & Movshon, 1992).

2.5.4 | Network imbalance indices

To quantify the extent of network imbalance between the MCN and DMN, we calculated the network imbalance indices (NII) as follows:

$$NII = \frac{|\beta_{MCN} + \beta_{DMN}|}{|\beta_{MCN}| + |\beta_{DMN}|}, \quad (2)$$

where β_{MCN} and β_{DMN} are the mean regional activity, or the mean interregional functional connectivity, of the MCN and DMN, respectively. As the MCN and DMN activities are anticorrelated, a large magnitude of NII indicates presence of severe network imbalance, and vice versa.

2.5.5 | Functional connectivity analyses

The ROI-wise functional connectivity analyses were custom-made (https://github.com/BNUDM/Functional_Connectivity_Analysis),

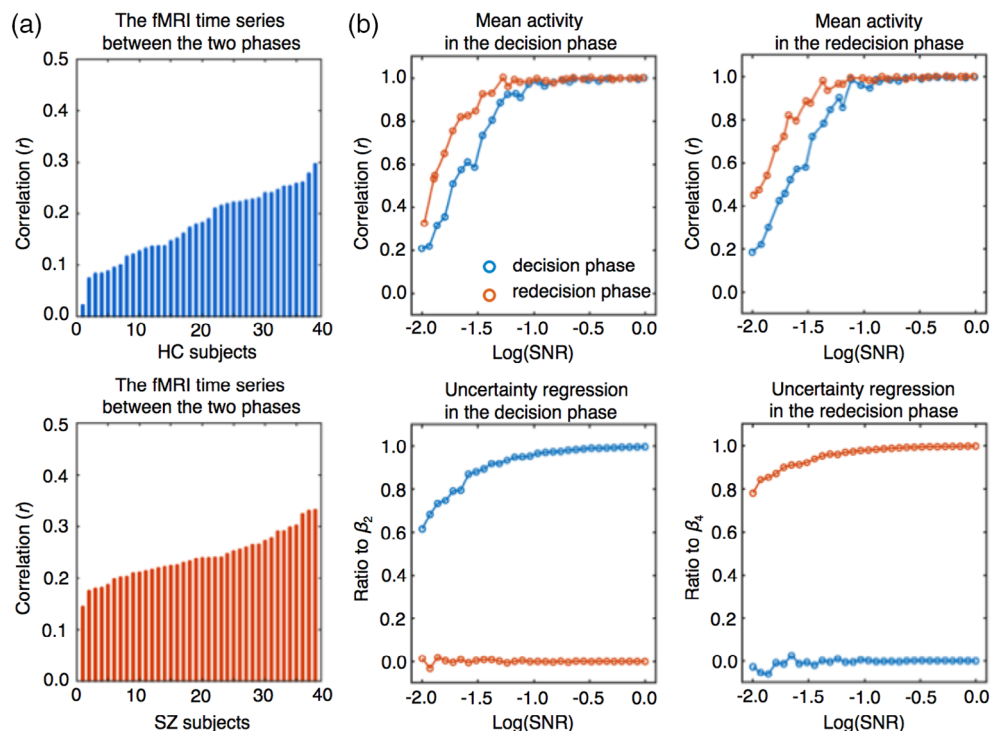


FIGURE 2 Reliable estimates of the neural activities in the decision and redecision phases. (a) The fMRI time series of the two phases were partially collinear in HC and SZ. (b) The estimated mean activity was highly correlated with the true value for each phase. The decision uncertainty modulation effects were largely close to the true values when the modulation effect occurred to either phase

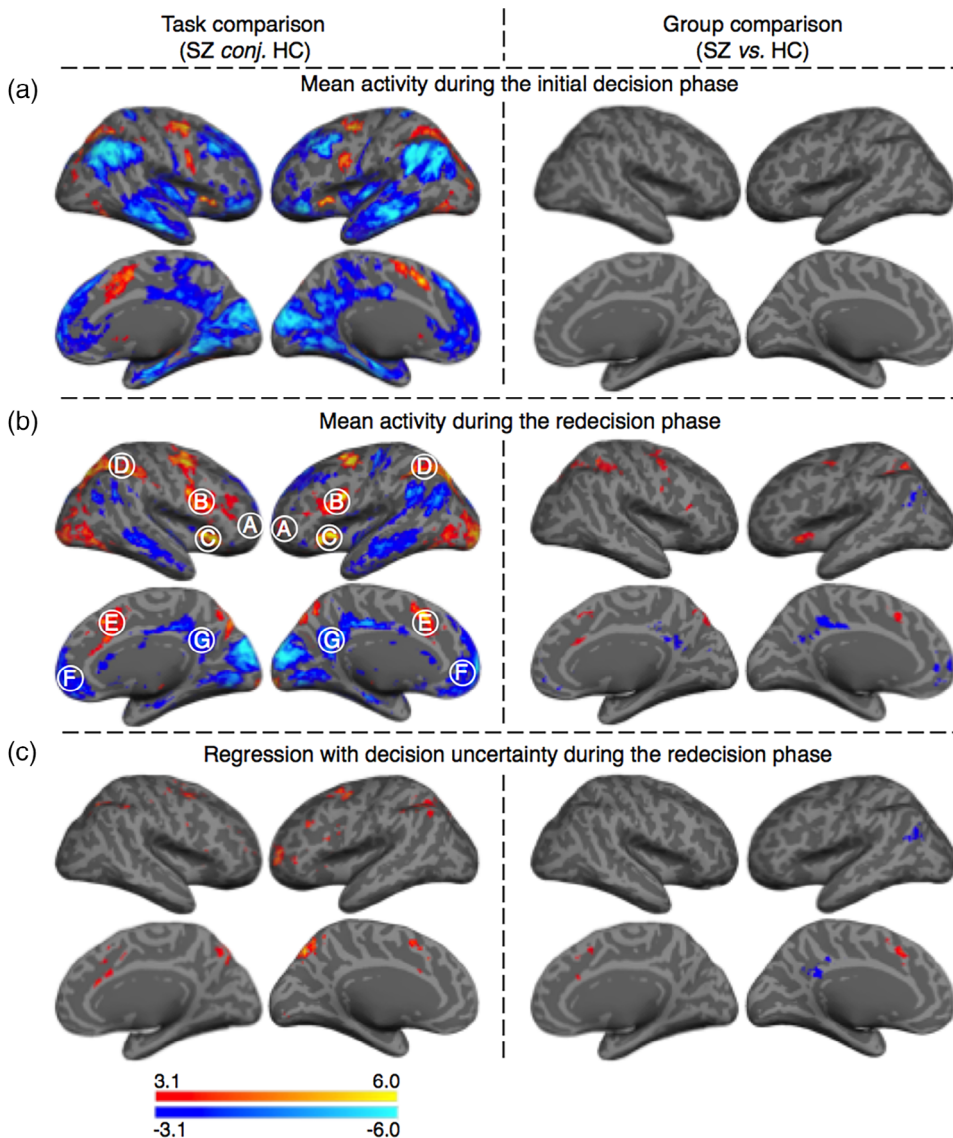


FIGURE 3 The disruptions of the MCN and DMN during uncertainty monitoring. (a) The activations were similar between HC and SZ during the first decision-making phase. (b) The activations were significantly different between HC and SZ during the redecision phase in the task trials in comparison to the same phase in the control trials. (c) The activations in regression with the decision uncertainty level were significantly different between HC and SZ during the redecision phase. All maps were obtained with the threshold as $z = 3.1$, $p < .05$, FDR corrected. Red-yellow colors indicate positive activations, and blue-green colors indicate negative activations. A, frontopolar cortex (FPC); B, dorsolateral prefrontal cortex (dlPFC); C, anterior insular cortex (AIC); D, anterior inferior parietal lobe (aIPL); E, anterior cingulate cortex (dACC); F, ventromedial prefrontal cortex (vmPFC); G, posterior cingulate cortex (PCC)

specifically for the task-based fMRI data. After the mean activity and the components associated with decision uncertainty, RT and their interactions were removed out, the residual time series of each ROI were averaged across the voxels of the ROI and segmented into individual trials regarding the task and control conditions, respectively. Each segmented trial was modeled using a single regressor during the redecision phase convolved with the canonical HRF, and the correlation coefficient was obtained across trials between a pair of ROIs in the same condition.

2.6 | Statistical tests

For the comparison of the behavioral data and neural activities between the two groups, the two-tailed two-sample t test was used. For the correlations between two variables, the correlation coefficients were fisher's r -to- t transformed and tested using the two-tailed t test. The statistical maps were described above.

3 | RESULTS

3.1 | Metacognitive abilities of decision uncertainty monitoring

We employed the “decision-redecision” paradigm in making decisions on the same problem twice in each trial (Figure 1a), to separate the metacognitive process during the redecision phase from the decision-making process during the first decision-making phase. The task difficulty was quite different between the two groups (stimulus coherence; SZ: $16.8 \pm 10.2\%$; HC: $8.8 \pm 4.3\%$, two-tailed two-sample t test, $t_{76} = 4.85$, $p = 2.2 \times 10^{-5}$, Figure 1b), whereas the performance accuracy in the first decision-making was kept largely same between the two groups by virtue of the staircase procedure (mean \pm standard deviation; SZ: $50.6 \pm 11.5\%$; HC: $51.7 \pm 7.3\%$, two-tailed two-sample t test, $t_{76} = 0.33$, $p = .37$, Figure 1c), The RTs between the two groups were not different in both decision-making phases (two-tailed two-sample t test, $t_{76} = 1.4$, $p = .10$ in the first decision-making; $t_{76} = 0.85$, $p = .23$ in the redecision). The reported decision uncertainty was

inversely proportional to the actual performance accuracy for both decision-making phases in HC, but became less discriminated in SZ (two-tailed two-sample *t* test on the Pearson's correlation coefficients, $t_{76} = 3.35$, $p = 9.2 \times 10^{-4}$, Figure 1d). Furthermore, the reported decision uncertainty was positively correlated with RT for both decision-making phases in HC, but became trivial in SZ (two-tailed two-sample *t* test, $t_{76} = 2.86$, $p = .0034$, Figure 1e). As the confidence ratings that SZ reported were also almost four in the control condition, it was unlikely that SZ randomly reported their confidence ratings in the task. Thus, SZ became insensitive to decision uncertainty in comparison to HC. To quantitatively calibrate the metacognitive ability of decision uncertainty monitoring for each subject, we calculated the behavioral AUC (b-AUC) on the basis of the reported confidence (Figure 1f). Although the b-AUCs in SZ were significantly higher than the chance level (0.5, dotted line; two-tailed one-sample *t* test, $t_{37} = 2.72$, $p = .0062$), but much lower than those of HC accompanying both decision-making phases (Figure 1g, two-tailed two-sample *t* test, $t_{76} = 3.82$, $p = .00049$). Despite the fact that the reported decision uncertainty was reduced equally by redecision in both groups [analysis of variance (ANOVA), $F_{[1, 111]} = 1.63$, $p = .20$, Figure 1h], accuracy improvement by redecision was also much lower in SZ than HC (Figure 1c), especially when uncertainty reduction was greater (Figure 1i, two-tailed two-sample *t* test, $t_{76} = 4.56$, $p = 5.4 \times 10^{-5}$ after Bonferroni correction). Together, SZ showed metacognitive deficit in both metacognitive monitoring of decision uncertainty and metacognitive control of decision adjustment.

3.2 | Neural networks associated with metacognitive monitoring

As metacognition automatically accompanies decision-making with decision uncertainty (Qiu et al., 2018), it is infeasible to temporally separate them by adding time jitters between the two events as conventionally used in the event-related task paradigms. Thereby, the fMRI activities of the two events in the GLM analyses should be partially collinear. This might result in confusions about the estimated neural activities in the two phases. To examine whether it is still feasible to separate their mean activities and the decision uncertainty modulation effects between the two phases, we made analyses on the simulation data that were generated from the exact same design matrix used for the subjects. Although the fMRI time series between the two phases were correlated in both groups (Pearson's $r = 0.1$ – 0.3 , Figure 2a), it is feasible to estimate the corresponding values that are highly correlated with the true values of the mean activities or largely close to the true modulation effects of the decision uncertainty for both phases (Figure 2b), when the SNR is reasonably as high as the normal cases in task fMRI data ($>1/30$).

The fMRI activities during the first decision-making phase did not differ between the two groups (Figure 3a). Both groups also showed very similar activity patterns during the redecision phase, in comparison to the same phase in the control condition (Figure 3b and Table 2). Significant activation in the MCN and significant

deactivation in the DMN were primarily observed for both groups. However, the strengths of fMRI activities in both the MCN and the DMN during the redecision phase were consistently smaller in SZ than HC (Figure 3b). Critically, the fMRI activities in the MCN during the redecision phase, but not during the first decision-making phase, positively correlated with the decision uncertainty levels, whereas the fMRI activities in the DMN negatively correlated with the decision uncertainty levels (Figure 3c and Table 3). The linear regression strengths in the two networks, particularly in dACC (peak MNI coordinate: $-6, 18, 42$) and posterior cingulate cortex (PCC, peak MNI coordinate: $0, -48, 22$), were much smaller in SZ (Figure 3c and Figure 4a), regardless of whether the decisions were correct or not (Figure 5).

3.3 | Neural representations of decision uncertainty sensitivity

To specifically examine the neural basis of the metacognitive deficit in decision uncertainty monitoring in SZ, we measured and compared the neural representations of decision uncertainty sensitivity in each subject of both groups, with reference to their behavioral uncertainty sensitivity (b-AUC). One form of the neural representations was the linear regression strength of fMRI activity with the decision uncertainty level; the other was the neural uncertainty sensitivity (n-AUC), a nonparametric measurement to examine the relationships between trial-by-trial fMRI activities and the correctness of the first decisions. The n-AUC in the brain areas critically associated with metacognition should match individual b-AUC in HC, and also quantitatively capture the metacognitive deficit in SZ.

Although the values of either neural representation in dACC positively correlated with b-AUCs in both groups, the neural representation strengths in dACC and PCC were consistently lower in SZ than HC (Figure 4b,c right columns, two-tailed two-sample *t* test, $ps < .01$). The n-AUCs in dACC were largely equivalent to the b-AUCs in HC (two-tailed one-sample *t* test, $t_{37} = 0.89$, $p = .19$, Figure 4c). This confirmed that the n-AUC was a reliable indicator of each subject's decision uncertainty sensitivity, and the dACC trial-by-trial neural activities represented the trial-by-trial decision uncertainty in HC. However, the n-AUCs in dACC were significantly lower than the corresponding b-AUCs in SZ (two-tailed one-sample *t* test, $t_{37} = 2.3$, $p = .012$, Figure 4c). In contrast, correlation between the values of each neural representation and b-AUCs in PCC was significantly negative in HC (two-tailed one-sample *t* test, $ps < .05$), but it became trivial in SZ (Figure 4b,c).

3.4 | Network imbalance correlates of clinical symptoms

The local hypo-activity in the MCN and DMN regions during metacognition, however, did not consistently correlate with clinical symptoms. We then examined the network properties between the MCN

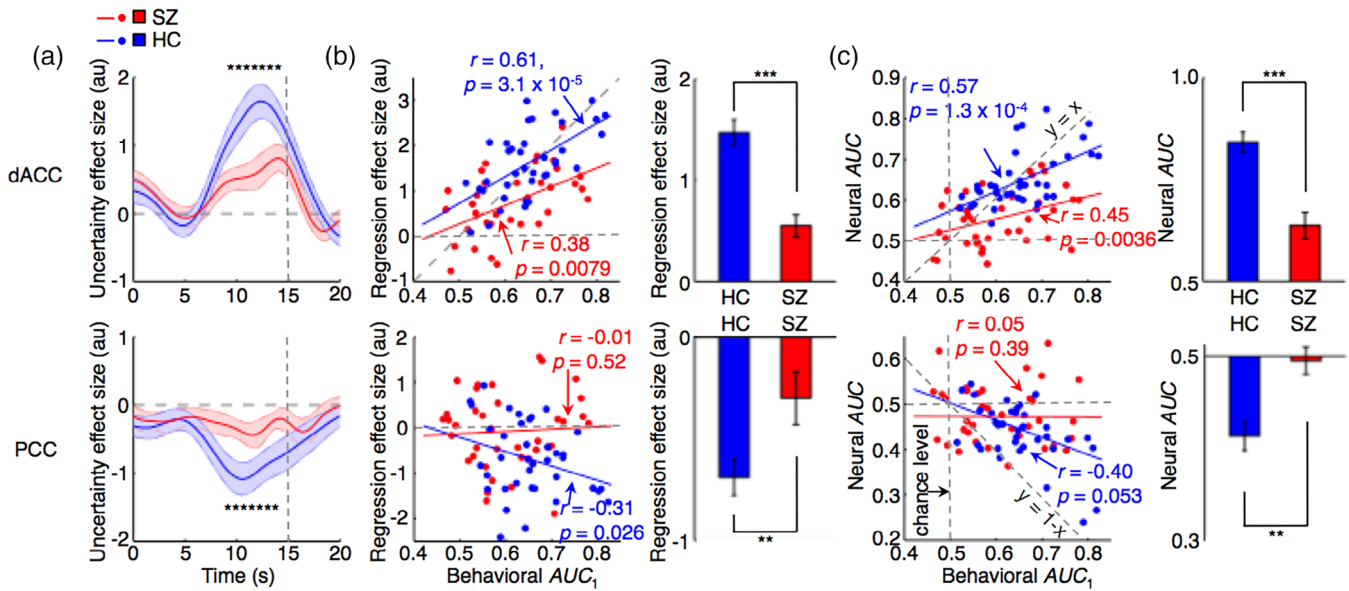


FIGURE 4 Aberrance of dACC and PCC regional activities in association with the metacognitive deficit of uncertainty monitoring. (a) Neural activities in dACC and PCC in regression with the decision uncertainty level were significantly different between HC and SZ. Time zero indicates the stimulus presentation in the first decision-making. (b) Regression effect size with the decision uncertainty level as a function of b-AUC (behavioral uncertainty sensitivity measured by the area under the type-2 ROC curve constructed by the decision uncertainty) on the first decisions (solid lines indicate the regressions across the subjects of groups and the dashed lines indicate the regressions across all subjects). Significant difference of the regression effect size between HC and SZ (right column). (c) n-AUC (neural uncertainty sensitivity measured by the area under the type-2 ROC curve constructed by the trial-by-trial neural activities) as a function of b-AUC on the first decisions. Significant difference of n-AUC between HC and SZ (right column). ** $p < .01$, *** $p < .001$. Error bars and shadings indicate standard error of the mean across subjects

and DMN that could be associated with clinical symptoms. The regional activities in the DMN were consistently anticorrelated with the regional activities in the MCN during the redecision phase (Figure 6a). The activations in the MCN and the deactivations in the DMN were proportional to each other, and were kept at a good balance in HC (Figure 6a). However, this network balance was disrupted in SZ.

To quantify the extent of network imbalance in SZ, we calculated two types of network imbalance indices (NII). One was measured by linear regression strength of regional activities with the decision uncertainty level, the other measured by functional connectivity within and between the MCN and DMN. Both NIIs were larger in SZ [Kolmogorov-Smirnov (K-S) test, $p = .0078$, Figure 6b; $p = .0065$, Figure 7a]. Importantly, both NIIs in SZ highly correlated with total scores of negative symptoms (two-tailed one-sample t test, $r = 0.68$, $t_{37} = 5.7$, $p = 1.4 \times 10^{-6}$, Bonferroni-corrected, Figure 6c; $r = 0.64$, $t_{37} = 5.1$, $p = 4.6 \times 10^{-6}$, Figure 7b), but did not correlate with total scores of positive symptoms (two-tailed one-sample t test, $r = -0.26$, $t_{37} = 1.6$, $p = .10$, Figure 6d). The NIIs in SZ also highly correlated with deficits in accuracy improvement in SZ (two-tailed one-sample t test, $r = -0.46$, $t_{37} = 3.7$, $p = .0018$), whereas the correlation between negative symptoms and accuracy improvement was trivial (two-tailed one-sample t test, $r = 0.12$, $t_{37} = 0.74$, $p = .23$).

Alternations of network balance between the two disrupted networks in SZ were also evident in the condition that did not need decision uncertainty monitoring (i.e., confidence rating = 4). In this

condition, the two networks were decoupled in HC, but remained entangled in SZ. HC reversely showed reliable biases of network balance, which were significantly larger than SZ (K-S test, $p = 5.6 \times 10^{-4}$, Figure 6e). Contrastingly, the strength of excessive fMRI activities across the MCN and DMN in SZ did not correlate with the total score of negative symptoms (two-tailed one-sample t test, $r = 0.02$, $t_{37} = 0.12$, $p = .45$, Figure 6f), but positively correlated with the total score of positive symptoms (two-tailed one-sample t test, $r = 0.57$, $t_{37} = 4.3$, $p = 1.2 \times 10^{-4}$, Bonferroni-corrected, Figure 6g).

4 | DISCUSSION

4.1 | Hypo-activity in the MCN and the metacognitive deficit

Although SZ had also deficits in motion perception (Martinez et al., 2018), utilizing a staircase procedure to control performance accuracy for each subject, this study was able to specifically investigate the metacognitive deficit of decision uncertainty monitoring in SZ. In addition, the “decision-redecision” paradigm in making decisions on the same problem twice in each trial could separate the neural system merely involving in the metacognitive process that merely occurred during the redecision phase from that of the decision-making process that also occurred during the first decision-making phase. The newly involving fMRI activities during the redecision phase in comparison to

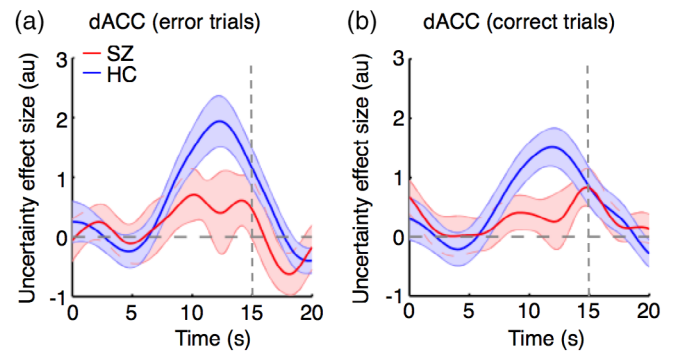
TABLE 2 Activations between the task and control trials during the redecision phase

Anatomical region	Hemispheres	MNI coordinate (x, y, z)	Maximum z value
Conjunction across healthy subjects and schizophrenia patients			
Lateral Frontopolar cortex (IFPC)	L	-34, 58, 6	3.88
Precentral Gyrus	L	-30, -2, 48	5.54
	R	28, -4, 52	5.55
Inferior frontal junction (IFJ)	L	-50, 6, 20	5.63
	R	52, 10, 32	5.28
Anterior inferior parietal lobe (aIPL)	L	-34, -50, 46	5.03
	R	40, -42, 44	5.35
Dorsal anterior cingulate cortex (dACC)	-	2, 14, 46	5.63
Anterior insular cortex (aIC)	L	-30, 22, 0	5.85
	R	32, 22, 2	5.86
Ventromedial prefrontal cortex (vmPFC)	-	-8, 44, -6	4.56
Posterior cingulate cortex (PCC)	-	-4, -52, 24	4.69
Contrast between healthy subjects and schizophrenia patients			
Precentral Gyrus	L	-32, -6, 46	3.76
	R	34, 0, 42	3.78
IFJ	R	58, 18, 20	4.01
aIPL	L	-32, -58, 50	3.91
	R	38, -44, 48	3.92
dACC	-	-6, 16, 38	4.45
aIC	L	-28, 24, -6	3.84
vmPFC	-	0, 46, -8	3.19
PCC	-	-9, -56, 24	3.24

those during the first decision-making phase are not necessarily related to metacognition, could be generally associated with the second decision-making. However, the fMRI activities in the MCN predominately occurring during the redecision phase were subject to the decision uncertainty levels on the preceding decisions, similar to the findings in the previous studies (Fleming et al., 2012; Morales et al., 2018; Qiu et al., 2018; Wan et al., 2016). Specifically, we here found that metacognitive abilities of decision uncertainty monitoring were lower, and the strengths of fMRI activities in the MCN, especially in dACC, were consistently much more reduced in SZ than HC. The selective reduction of fMRI activities in the MCN during redecision, rather than the first decision-making (Figure 3a,b), indicates that these abnormal neural activities in SZ were selectively associated with

TABLE 3 Activations correlated with decision uncertainty during the redecision phase

Anatomical region	Hemispheres	MNI coordinate (x, y, z)	Maximum z value
Conjunction across healthy subjects and schizophrenia patients			
IFPC	L	-30, 60, 10	4.12
Precentral Gyrus	L	-32, 2, 56	4.30
	R	26, 4, 52	4.03
dIPFC	L	-48, 34, 26	3.83
	R	50, 32, 28	3.45
IFJ	L	-50, 12, 30	3.34
	R	54, 12, 30	3.68
aIPL	L	-46, -48, 44	3.73
	R	50, -40, 46	3.37
dACC	-	0, 18, 36	4.59
aIC	L	-38, 18, -4	3.94
	R	32, 20, 2	3.10
Contrast between healthy subjects and schizophrenia patients			
dACC	-	-6, 18, 42	3.63
PCC	-	0, -48, 22	3.69

**FIGURE 5** Regional activity in dACC similarly regressed with decision uncertainty in both the error trials (a) and the correct trials (b) (differently significant between HC and SZ). Time zero indicates the stimulus presentation in the first decision-making. Shadings indicate standard error of the mean across subjects

metacognition, rather than decision-making per se. Further, hypoactivity in these regions in individual SZ highly correlated with their extents of metacognitive deficit, but not the clinical symptoms.

We showed that the fMRI activities in the MCN proportionally changed with the decision uncertainty level, specifically in dACC. The trial-by-trial neural activity (n-AUC) quantitatively characterized the individual metacognitive ability of decision uncertainty monitoring (b-AUC), underlying the metacognitive deficit in SZ. As the MCN is commonly associated with metacognition accompanying a variety of decision-making tasks (Fleming et al., 2012; Morales et al., 2018; Qiu et al., 2018; Wan et al., 2016), the association of hypo-activity in the

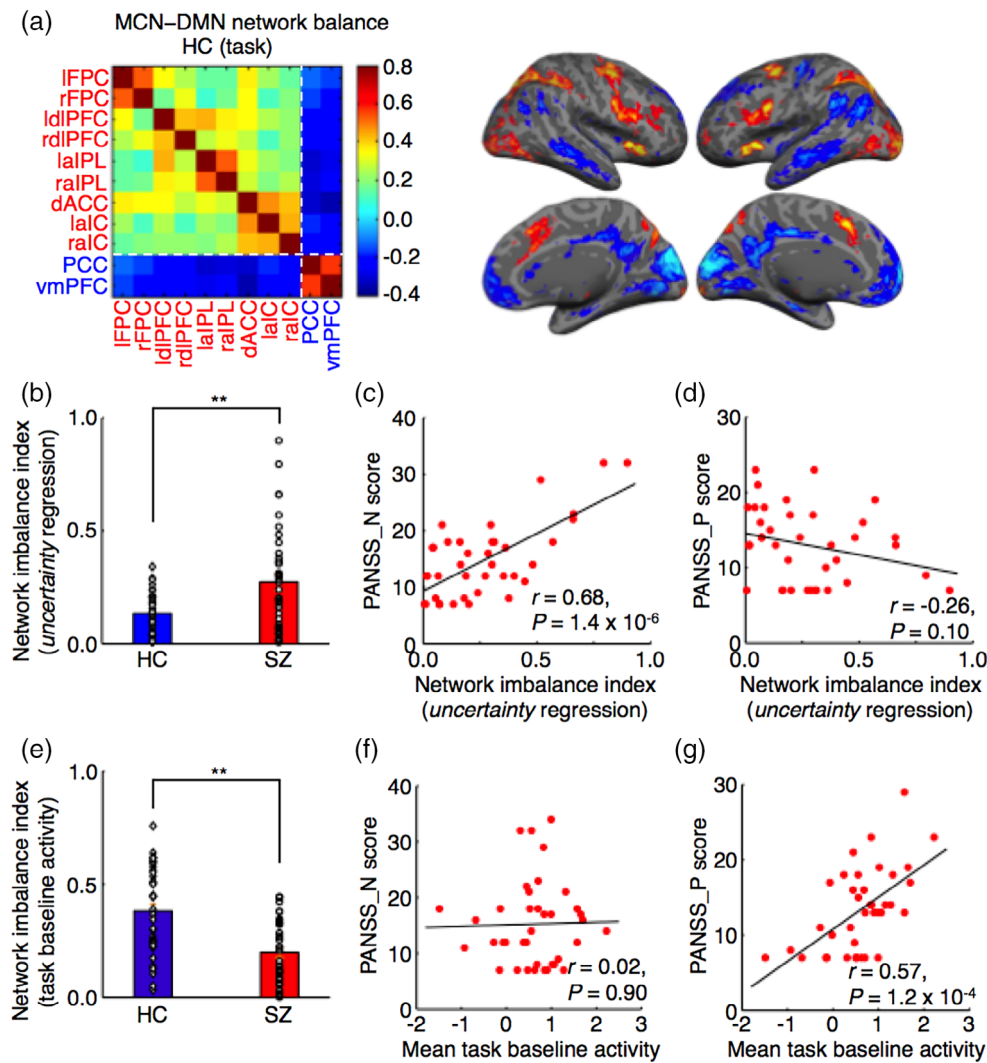


FIGURE 6 Alterations of network balance between the disrupted MCN and DMN in association with clinical symptoms. (a) The anticorrelation between the MCN and DMN. The correlation coefficients between the regional activities within the MCN and DMN were positive, but were negative across the two networks in HC during the redecision phase. The activation maps are the same as in Figure 2b. (b) Network imbalance index measured by regional activity strength during metacognition in SZ was significantly higher than that in HC. (c) Network imbalance index during metacognition positively correlated with total PANSS score of negative symptoms. (d) Network imbalance index during metacognition did not correlate with total PANSS score of positive symptoms. (e) Network imbalance index measured by regional activity strength in the task condition that did not require uncertainty monitoring (task baseline activity) in SZ was significantly lower than that in HC. (f) The excessive neural activity across the MCN and DMN did not correlate with the total PANSS score of negative symptoms. (g) The excessive neural activity across the MCN and DMN positively correlated with the total PANSS score of positive symptoms. $**p < .01$. Error bars indicate standard error of the mean across subjects

MCN with the metacognitive deficit in SZ could be general. The hypo-activity in the MCN was consistent with the replicated findings of structural and functional abnormalities in this network in SZ (Brugger & Howes, 2017; Carter et al., 2001; Goodkind et al., 2015; Kerns et al., 2005; Pettersson-Yeo et al., 2011). For instance, dACC has been previously reported to show hypo-activity in error or conflict monitoring tasks in SZ (Carter et al., 2001; Kerns et al., 2005). Extended to these findings, the current study showed that the subjects evaluated their own mental states of decision uncertainty via the internal signals for both correct and incorrect trials, rather than through external feedback (Figure 5). The abnormality of monitoring one's own internal mental state is a core feature of SZ. The current

findings suggest that the MCN, specifically dACC, should be critically associated with this deficit.

4.2 | Hypo-activity in the DMN and the metacognitive deficit

The DMN suppression during metacognition is normally induced by the MCN activation in HC. It is thereby expected that the DMN suppression should also be weakened in SZ. However, we found that reduction of DMN suppression did not simply mirror hypo-activity in the MCN. In some SZ patients, the PCC activities were even positively

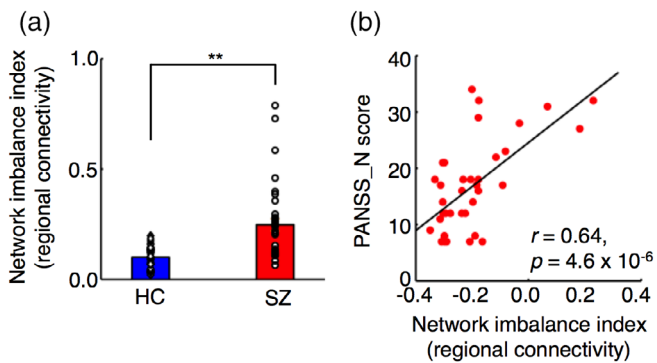


FIGURE 7 Network imbalance between the MCN and DMN measured by interregional functional connectivity. (a) Network imbalance measured by interregional functional connectivity within and between the MCN and DMN in SZ was significantly higher than that in HC. (b) Network imbalance index measured by interregional functional connectivity positively correlated with total PANSS score of negative symptoms. $**p < .01$

correlated with the decision uncertainty levels, and the corresponding n-AUCs were abnormally larger than 0.5, similar to what were seen in the MCN regions (Figure 3). This evidence implies that the DMN in SZ might also contribute to metacognition as the MCN did, thus the functions of the two networks became ambiguous in SZ (Baker et al., 2014). Hence, the metacognitive deficit of decision uncertainty monitoring in SZ should be associated with disruptions in both the MCN and DMN.

4.3 | Network imbalance between the MCN and DMN and clinical symptoms

Network balance between the two disrupted networks during the redecision phase, was significantly altered in SZ, and severely deviated from that in HC. Critically, the extents of network imbalance were selectively associated with negative symptoms in SZ, whereas the strengths of excessive fMRI activities in the task condition that did not elicit decision uncertainty were complementarily associated with positive symptoms. Thus, the network imbalance was a crucial indicator of clinical symptoms in SZ. To our knowledge, this is the first report of neural linkage between the metacognitive deficits and clinical symptoms in SZ. Our findings that the network imbalance between the MCN and DMN rather than hypo-activity in these brain regions underpinned the SZ symptoms provide important implications for the therapeutic development.

The results that alternations of anticorrelations between the disrupted MCN and DMN were associated with both negative symptoms and deficits in accuracy improvement in SZ, implicates that both negative symptoms and impaired functional outcomes might be commonly induced by alternations in network balance. It is possible that abnormality of network balance in SZ impairs metacognitive control, which results in lower levels of accuracy improvement (Figure 1e).

Consequently, frequent failures to obtain positive outcomes impede their engagement in everyday activities. Alternately, it is also possible that intrinsically lower levels of motivation or volition, which constitute a critical feature of the negative symptoms, result in lower levels of inclination to improve their performance (Gorissen, Sanz, & Schmand, 2005; Green, Horan, Barch, & Gold, 2015).

The anticorrelated fMRI activities across the two disrupted networks in SZ reversely remained high when uncertainty monitoring was not elicited during the task. The regional activity strength in this condition was selectively associated with positive symptoms, such as delusions and hallucinations. Probably, excessive fMRI activity in the MCN and DMN in the condition that did not evoke metacognitive monitoring and metacognitive control in reality might adversely generate unrealistic and pathologic beliefs on one's own mental states. This notion is consistent with the previous proposal that hallucinations and delusions are more generated by the abnormal resting-states (Northoff & Qin, 2011). Furthermore, our results were consistent with previous findings on resting-state fMRI that intrinsic connectivity strength was weakened within each of the internal networks, but was strengthened between the networks (Pettersson-Yeo et al., 2011; Stephan, Friston, & Frith, 2009).

Failures of flexible coordination between the two disrupted networks of the MCN and DMN might impair cognitive flexibility in the face of different metacognitive demands (Cole et al., 2013). Alternations of anticorrelation between the two disrupted networks are consistent with the disconnectivity hypothesis in SZ (Stephan et al., 2009), presumably caused by local excitation-inhibition imbalance (Moghaddam & Javitt, 2012). So far, the neural mechanisms underlying anticorrelation between the MCN and DMN have remained largely unclear. It has been proposed that the SN, consisting of dACC and anterior insular cortex (aIC), played a critical role in modulating the central attentional network (also a frontoparietal control network) and DMN (Menon, 2011). Nevertheless, dACC and aIC per se belong to a sub-network of the MCN. Therefore, there should exist an independent neural locus or neural network that mediate the anticorrelation between the MCN and DMN.

While the metacognitive deficits in SZ have been shown to be clinically associated with both negative and positive symptoms, our findings implicate that these associations could be complicated and multifaceted. The dominant hypo-activity in the MCN and DMN during metacognition complied with the metacognitive deficit in decision uncertainty monitoring, but was not associated with clinical symptoms. Instead, the network imbalance between the two disrupted networks was closely associated with clinical symptoms. Given the facts that some healthy individuals who may have also low metacognitive capabilities in decision uncertainty monitoring but lack the obvious SZ clinical symptoms, it is reasonable to believe that hypo-activity in the MCN and DMN could not directly cause SZ symptoms. In contrast, the misattribution of the MCN and DMN functions during metacognition, as indicated by the network imbalance, might be the critical factor to influence the SZ symptoms. However, it remains intrigued whether hypo-activity in the MCN and DMN results in network imbalance between the two networks, or vice versa.

4.4 | Limitations

Several limitations of this study merit comments. First, differences in medication could present a potential confound. However, there were not any significant correlations between medication equivalent dosage, or time post-diagnosis, with the metacognitive ability, network imbalance, or negative or positive symptoms. Second, the measure of insight such as the Beck Cognitive Insight Scale (BCIS, Beck et al., 2004) and the Scale to Assess Unawareness of Mental Disorder (SUMD, Amador et al., 1994) were not administered in the current study. Future research needs to explore the relationship between the metacognition deficit of cognitive insight and the impairment of clinical insight. Third, metacognition in this study was constrained to monitoring and control of one's own cognitive processes, namely, metacognitive experiences. Other aspects of metacognition, particularly relevant to metacognitive knowledge, should be further explored.

Lastly, while this study focused on investigating the neural mechanisms of metacognitive deficit in decision uncertainty monitoring in SZ, it is possible that these findings are widespread in psychosis (McTeague et al., 2017; Shanmugan et al., 2016). The metacognitive deficits are commonly reported phenomena across different mental illnesses (Luther et al., 2016). Disruptions in the MCN and DMN have also been reported in other psychotic disorders (Rose, Simonotto, & Ebmeier, 2006; Sheline et al., 2009). Further investigations on this issue should increase general understanding of the neuropathology across the spectrum of psychosis.

5 | CONCLUSION

The current study is the first report identifying neural bases underpinning the relationships between the metacognitive deficit and clinical symptoms in SZ. The metacognitive deficit was associated with hypoactivity in both the MCN and the DMN, and alternations of balance between the two disrupted networks were associated with clinical symptoms. Our findings suggest that disruptions of the MCN and DMN should contribute to the SZ neuropathology, and that balance between the two disrupted networks might be used as a biomarker in gauging efficacy for the therapeutic development.

ACKNOWLEDGMENTS

We thank L. Qiu, X. Zhang, Z. Xiao, S. Wang, and Y. Cai for technical assistance. This study was funded by the National Natural Science Foundation of China (No. 31471068), Key Program for International S&T Cooperation Projects of China (MOST, 2016YFE0129100), the Fundamental Research Funds for the Central Universities (2017EYT33) and the Thousand Young Talents Program of China. The funding sources had no role in the design and conduct of the study.

CONFLICT OF INTERESTS

The authors declare no conflict of interest.

DATA AVAILABILITY STATEMENT

The data that support the findings of this study are available from the corresponding author upon reasonable request.

ORCID

Xiaohong Wan  <https://orcid.org/0000-0002-6472-1435>

REFERENCES

- Amador, X., Strauss, D., Yale, S., Flaum, M., Endicott, J., & Gorman, J. (1993). Assessment of insight in psychosis. *American Journal of Psychiatry*, *150*, 873–879.
- Amador, X. F., Flaum, M., Andreasen, N. C., Strauss, D. H., Yale, S. A., Clark, S. C., & Gorman, J. M. (1994). Awareness of illness in schizophrenia and schizoaffective and mood disorders. *Archives of General Psychiatry*, *51*, 826–836.
- Amador, X. F., Strauss, D. H., Yale, S. A., & Gorman, J. M. (1991). Awareness of illness in schizophrenia. *Schizophrenia Bulletin*, *17*, 113–132.
- Anticevic, A., Cole, M. W., Murray, J. D., Corlett, P. R., Wang, X.-J., & Krystal, J. H. (2012). The role of default network deactivation in cognition and disease. *Trends in Cognitive Sciences*, *16*, 584–592.
- Baker, J. T., Holmes, A. J., Masters, G. A., Yeo, B. T. T., Krienen, F., Buckner, R. L., & Öngür, D. (2014). Disruption of cortical association networks in schizophrenia and psychotic bipolar disorder. *JAMA Psychiatry*, *71*, 109–118.
- Beck, A. T., Baruch, E., Balter, J. M., Steer, R. A., & Warman, D. M. (2004). A new instrument for measuring insight: The Beck cognitive insight scale. *Schizophrenia Research*, *68*, 319–329.
- Behrens, T. E. J., Woolrich, M. W., Walton, M. E., & Rushworth, M. F. S. (2007). Learning the value of information in an uncertain world. *Nature Neuroscience*, *10*, 1214–1221.
- Britten, K. H., Shadlen, M. N., Newsome, W. T., & Movshon, J. A. (1992). The analysis of visual motion: A comparison of neuronal and psychophysical performance. *The Journal of Neuroscience*, *12*, 4745–4765.
- Brugger, S. P., & Howes, O. D. (2017). Heterogeneity and homogeneity of regional brain structure in schizophrenia: A meta-analysis. *JAMA Psychiatry*, *74*, 1104–1111.
- Buchy, L., Stowkowy, J., MacMaster, F. P., Nyman, K., & Addington, J. (2015). Meta-cognition is associated with cortical thickness in youth at clinical high risk of psychosis. *Psychiatry Research: Neuroimaging*, *233*, 418–423.
- Carpenter, W. T., Strauss, J. S., & Bartko, J. J. (1973). Flexible system for the diagnosis of schizophrenia: Report from the WHO international pilot study of schizophrenia. *Science*, *182*, 1275–1278.
- Carter, C. S., MacDonald, A. W., Ross, L. L., & Stenger, V. A. (2001). Anterior cingulate cortex activity and impaired self-monitoring of performance in patients with schizophrenia: An event-related fMRI study. *American Journal of Psychiatry*, *158*, 1423–1428.
- Cole, M. W., Reynolds, J. R., Power, J. D., Repovs, G., Anticevic, A., & Braver, T. S. (2013). Multi-task connectivity reveals flexible hubs for adaptive task control. *Nature Neuroscience*, *16*, 1348–1355.
- Danion, J.-M., Gokalsing, E., Robert, P., Massin-Krauss, M., & Bacon, E. (2001). Defective relationship between subjective experience and behavior in schizophrenia. *American Journal of Psychiatry*, *158*, 2064–2066.
- Dunlosky, J., & Metcalfe, J. (2009). *Metacognition* (1st ed.). Thousand Oaks: Sage Publications Inc.
- Flavell, J. H. (1979). Metacognition and cognitive monitoring: A new area of cognitive-developmental inquiry. *American Psychologist*, *34*, 906–911.
- Fleming, S. M., Huijgen, J., & Dolan, R. J. (2012). Prefrontal contributions to metacognition in perceptual decision making. *Journal of Neuroscience*, *32*, 6117–6125.

- Fox, M. D., Snyder, A. Z., Vincent, J. L., Corbetta, M., & Raichle, M. E. (2005). The human brain is intrinsically organized into dynamic, anticorrelated functional networks. *Proceedings of the National Academy of Sciences*, *102*, 9673–9678.
- Francis, M. M., Hummer, T. A., Leonhardt, B. L., Vohs, J. L., Yung, M. G., Mehdiyou, N. F., ... Breier, A. (2017). Association of medial prefrontal resting state functional connectivity and metacognitive capacity in early phase psychosis. *Psychiatry Research: Neuroimaging*, *262*, 8–14.
- Goodkind, M., Eickhoff, S. B., Oathes, D. J., Jiang, Y., Chang, A., Jones-Hagata, L. B., ... Etkin, A. (2015). Identification of a common neurobiological substrate for mental illness. *JAMA Psychiatry*, *72*, 305–315.
- Gorissen, M., Sanz, J. C., & Schmand, B. (2005). Effort and cognition in schizophrenia patients. *Schizophrenia Research*, *78*, 199–208.
- Green, M. (1996). What are the functional consequences of neurocognitive deficits in schizophrenia? *American Journal of Psychiatry*, *153*, 321–330.
- Green, M. F., Horan, W. P., Barch, D. M., & Gold, J. M. (2015). Effort-based decision making: A novel approach for assessing motivation in schizophrenia. *Schizophrenia Bulletin*, *41*, 1035–1044.
- Gusnard, D. A., & Raichle, M. E. (2001). Searching for a baseline: Functional imaging and the resting human brain. *Nature Reviews Neuroscience*, *2*, 685–694.
- Harrison, B. J., Yücel, M., Pujol, J., & Pantelis, C. (2007). Task-induced deactivation of midline cortical regions in schizophrenia assessed with fMRI. *Schizophrenia Research*, *91*, 82–86.
- Kay, S. R., Fiszbein, A., & Opler, L. A. (1987). The positive and negative syndrome scale (PANSS) for schizophrenia. *Schizophrenia Bulletin*, *13*, 261–276.
- Kerns, J. G., Cohen, J. D., MacDonald, A. W., Johnson, M. K., Stenger, V. A., Aizenstein, H., & Carter, C. S. (2005). Decreased conflict- and error-related activity in the anterior cingulate cortex in subjects with schizophrenia. *American Journal of Psychiatry*, *162*, 1833–1839.
- Kiani, R., & Shadlen, M. N. (2009). Representation of confidence associated with a decision by neurons in the parietal cortex. *Science*, *324*, 759–764.
- Levitt, H. (1971). Transformed up-down methods in psychoacoustics. *The Journal of the Acoustical Society of America*, *49*, 467–477.
- Luther, L., Firmin, R. L., Minor, K. S., Vohs, J. L., Buck, B., Buck, K. D., & Lysaker, P. H. (2016). Metacognition deficits as a risk factor for prospective motivation deficits in schizophrenia spectrum disorders. *Psychiatry Research*, *245*, 172–178.
- Lysaker, P., & Bell, M. (1994). Insight and cognitive impairment in schizophrenia: Performance on repeated administrations of the Wisconsin card sorting test. *Journal of Nervous and Mental Disease*, *182*, 656–660.
- Mannell, M. V., Franco, A. R., Calhoun, V. D., Cañive, J. M., Thoma, R. J., & Mayer, A. R. (2010). Resting state and task-induced deactivation: A methodological comparison in patients with schizophrenia and healthy controls. *Human Brain Mapping*, *31*, 424–437.
- Martinez, A., Gaspar, P. A., Hillyard, S. A., Andersen, S. K., Lopez-Calderson, J., Corcoran, C. M., & Javitt, D. C. (2018). Impaired motion processing in schizophrenia and the attenuated psychosis syndrome: Etiological and clinical implications. *American Journal of Psychiatry*, *175*, 424–437.
- McLeod, H. J., Gumley, A. I., MacBeth, A., Schwannauer, M., & Lysaker, P. H. (2004). Metacognitive functioning predicts positive and negative symptoms over 12 months in first episode psychosis. *J Psych Res*, *54*, 109–115.
- McTeague, L. M., Huemer, J., Carreon, D. M., Jiang, Y., Eickhoff, S. B., & Etkin, A. (2017). Identification of common neural circuit disruptions in cognitive control across psychiatric disorders. *American Journal of Psychiatry*, *174*, 676–685.
- Menon, V. (2011). Large-scale brain networks and psychopathology: A unifying triple network model. *Trends in Cognitive Sciences*, *15*, 483–506.
- Metzack, P. D., Riley, J. D., Wang, L., Whitman, J. C., Ngan, E. T. C., & Woodward, T. S. (2012). Decreased efficiency of task-positive and task-negative networks during working memory in schizophrenia. *Schizophrenia Bulletin*, *38*, 803–813.
- Miyamoto, K., Osada, T., Setsuie, R., Takeda, M., Tamura, K., Adachi, Y., & Miyashita, Y. (2017). Causal neural network of metamemory for retrospection in primates. *Science*, *355*, 188–193.
- Moghaddam, B., & Javitt, D. (2012). From revolution to evolution: The glutamate hypothesis of schizophrenia and its implication for treatment. *Neuropsychopharmacology*, *37*, 4–15.
- Morales, J., Lau, H., & Fleming, S. M. (2018). Domain-general and domain-specific patterns of activity supporting metacognition in human prefrontal cortex. *Journal of Neuroscience*, *38*, 3534–3546.
- Moritz, S., & Woodward, T. S. (2006). Metacognitive control over false memories: A key determinant of delusional thinking. *Current Psychiatry Reports*, *8*, 184–190.
- Mumford, J. A., Turner, B. O., Ashby, F. G., & Poldrack, R. A. (2012). Decoupling BOLD activation in event-related designs for multivoxel pattern classification analyses. *NeuroImage*, *59*, 2636–2643.
- Nelson, T. O., & Narens, L. (1990). Metamemory: A theoretical framework and new findings. *Psychology of Learning & Motivation*, *26*, 125–173.
- Northoff, G., & Qin, P. (2011). How can the brain's resting state activity generate hallucinations? A 'resting state hypothesis' of auditory verbal hallucinations. *Schizophrenia Research*, *127*, 202–214.
- Pettersson-Yeo, W., Allen, P., Benetti, S., McGuire, P., & Mechelli, A. (2011). Dysconnectivity in schizophrenia: Where are we now? *Neuroscience & Biobehavioral Reviews*, *35*, 1110–1124.
- Qiu, L., Su, J., Ni, Y., Bai, Y., Zhang, X., Li, X., & Wan, X. (2018). The neural system of metacognition accompanying decision-making in the prefrontal cortex. *PLoS Biology*, *16*, e2004037.
- Rissman, J., Gazzaley, A., & D'Esposito, M. (2004). Measuring functional connectivity during distinct stages of a cognitive task. *NeuroImage*, *23*, 752–763.
- Robinson, D. G., Woerner, M. G., McMeniman, M., Mendelowitz, A., & Bilder, R. M. (2004). Symptomatic and functional recovery from a first episode of schizophrenia or schizoaffective disorder. *American Journal of Psychiatry*, *161*, 473–479.
- Rose, E. J., Simonotto, E., & Ebmeier, K. P. (2006). Limbic over-activity in depression during preserved performance on the n-back task. *NeuroImage*, *29*, 203–215.
- Shanmugan, S., Wolf, D. H., Calkins, M. E., Moore, T. M., Ruparel, K., Hopson, R. D., ... Satterthwaite, T. D. (2016). Common and dissociable mechanisms of executive system dysfunction across psychiatric disorders in youth. *American Journal of Psychiatry*, *173*, 517–526.
- Sheline, Y. I., Barch, D. M., Price, J. L., Rundle, M. M., Vaishnavi, S. N., Snyder, A. Z., ... Raichle, M. E. (2009). The default mode network and self-referential processes in depression. *Proceedings of the National Academy of Sciences*, *106*, 1942–1947.
- Smith, S. M., Jenkinson, M., Woolrich, M. W., Beckmann, C. F., Behrens, T. E. J., Johansen-Berg, H., ... Matthews, P. M. (2004). Advances in functional and structural MR image analysis and implementation as FSL. *NeuroImage*, *23*, S208–S219.
- Stephan, K. E., Friston, K. J., & Frith, C. D. (2009). Dysconnection in schizophrenia: From abnormal synaptic plasticity to failures of self-monitoring. *Schizophrenia Bulletin*, *35*, 509–527.
- Wan, X., Cheng, K., & Tanaka, K. (2016). The neural system of post-decision evaluation in rostral frontal cortex during problem solving tasks. *eNeuro*, *3*, e018816.
- Whitfield-Gabrieli, S., Thermenos, H. W., Milanovic, S., Tsuang, M. T., Faraone, S. V., McCarley, R. W., ... Seidman, L. J. (2009). Hyperactivity and hyperconnectivity of the default network in schizophrenia and in first-degree relatives of persons with schizophrenia. *Proceedings of the National Academy of Sciences*, *106*, 1279–1284.

- Yang, G. J., Murray, J. D., Wang, X.-J., Glahn, D. C., Pearlson, G. D., Repovs, G., ... Anticevic, A. (2016). Functional hierarchy underlies preferential connectivity disturbances in schizophrenia. *Proceedings of the National Academy of Sciences*, 113, E219–E228.
- Yeo, B. T. T., Krienen, F. M., Sepulcre, J., Sabuncu, M. R., Lashkari, L., Hollinshead, M., ..., Buckner, R. L. (2011). The organization of the human cerebral cortex estimated by intrinsic functional connectivity. *Journal of Neurophysiology*, 106, 1125–1165.

How to cite this article: Jia W, Zhu H, Ni Y, et al. Disruptions of frontoparietal control network and default mode network linking the metacognitive deficits with clinical symptoms in schizophrenia. *Hum Brain Mapp.* 2020;41:1445–1458. <https://doi.org/10.1002/hbm.24887>